Remote Sensing of Environment 221 (2019) 351–362

Contents lists available at ScienceDirect

Remote Sensing of Environment

journal homepage: www.elsevier.com/locate/rse

Mapping forest disturbance intensity in North and South Carolina using annual Landsat observations and field inventory data

Xin Tao[a,*], Chengquan Huang[b], Feng Zhao[b], Karen Schleeweis[c], Jeffrey Masek[d], Shunlin Liang[b]

[a] Department of Geography, University at Buffalo, The State University of New York, Buffalo, NY 14261, USA
[b] Department of Geographical Sciences, University of Maryland, College Park, MD 20742, USA
[c] Forest Inventory and Analysis, US Forest Service, Rocky Mountain Research Station, Ogden, UT, USA
[d] NASA Goddard Space Flight Center, Greenbelt, MD, USA

ARTICLE INFO

Keywords:
Disturbance intensity
Spectral disturbance magnitude
Landsat
Model
Validation

ABSTRACT

Disturbance and regrowth are vital processes in determining the roles of forest ecosystem in the carbon and biogeochemical cycles. Using time series observations, the vegetation change tracker (VCT) algorithm was designed to map the location, timing, and spectral magnitudes of forest disturbance events. While these spectral disturbance magnitudes are indicative of physical changes in tree cover or biomass, their quantitative relationships have yet to be established. This study focuses on estimating disturbance intensity as measured by percent basal area removal using spectral indices from the VCT algorithm over North and South Carolina. Repeat measurements on Forest Service Forest Inventory Analysis (FIA) ground plots, which provide changes in basal area between multiple dates at precise locations, are used for training and validation of the model. The overall R^2 between predicted disturbance intensity and reference data is 0.66, and cross-validation prediction uncertainty is 14% in North Carolina. Possible causes of this uncertainty could be site heterogeneity and the temporal offset between ground measurements and satellite observations. Results show the area of stand clearing disturbances remains relatively stable around 1143 $km^2\,yr^{-1}$ in North and South Carolina throughout the period of observations (1985–2015). The average amount of forest area affected by partial disturbance is much higher at 3287 $km^2\,yr^{-1}$. The area of partial disturbances has strong inter-annual variability with a high value of 6000 km^2 in 2007 and a low value of 1919 km^2 in 2013.

1. Introduction

Forests play important roles in many physical, chemical, and biological processes that affect hydrology, energy balance, carbon fluxes, and biogeochemical cycling of nutrients (Bonan, 2008), and provide a broad range of socio-ecological services important to the human being (Myers, 1997; Patterson and Coelho, 2009). While their distribution, structure, and composition have been and will continue to be shaped by disturbances (Burton et al., 2008), the impact of those disturbance events, such as carbon emission (Birdsey and Lewis, 2003; Houghton et al., 2012), habitat loss (Bengtsson et al., 2000; Slade et al., 2011), soil erosion or degradation (Bari and Smettem, 2006; Petranka et al., 1993; Schofield and Ruprecht, 1989), among others, can differ greatly depending on disturbance type and intensity (Chambers et al., 2007; Stueve et al., 2011). The nature of disturbance events in turn drives post-disturbance recovery and associated carbon source-sink dynamics (Frolking et al., 2009; Goetz et al., 2012; Meng et al., 2015). In North Carolina, for example, the amount of carbon transferred to the wood products pool can be modeled based on the area and intensity of forest harvest (Huang et al., 2015; Ling et al., 2016), which had large variations across North America (Masek et al., 2011). Improved assessment of forest disturbance is therefore important for advancing studies of climate change and other pressing environmental issues (Goward et al., 2008).

Since the launch of the first Landsat in 1972, Landsat imagery has been a major data source for disturbance analysis, providing sub-hectare details needed to characterize many natural and human driven change processes. Numerous algorithms have been developed for detecting disturbance occurrence using satellite observations acquired at multi-year intervals (Coppin et al., 2004; Hussain et al., 2013; Lu et al., 2004; Singh, 1989; Tewkesbury et al., 2015), and a number of forest change products have been generated at national (Huang et al., 2009c), continental (Masek et al., 2008), and global scales (Kim et al., 2014; Sexton et al., 2015; Townshend et al., 2012).

* Corresponding author.
E-mail address: xintao@buffalo.edu (X. Tao).

https://doi.org/10.1016/j.rse.2018.11.029
Received 30 May 2018; Received in revised form 12 November 2018; Accepted 20 November 2018

A comprehensive mapping approach that utilizes as many points in time as possible and characterizes disturbance magnitude and duration is ideal for earth science applications (Kennedy et al., 2014; Senf et al., 2015). The opening of the Landsat archive for no-cost access in 2008 (Woodcock et al., 2008) made it financially feasible to assemble biennial, annual, or even denser Landsat time series over large areas. It ushered a new era characterized by booming development of time series based disturbance mapping algorithms (Devries et al., 2015; Healey et al., 2018; Hermosilla et al., 2015a; Hermosilla et al., 2015b; Huang et al., 2010; Kennedy et al., 2010; Schmidt et al., 2015; Senf et al., 2017; Wulder et al., 2016; Zhu et al., 2012), some of which have demonstrated success at state (Hermosilla et al., 2015b; Li et al., 2009a, 2009b), regional (Kennedy et al., 2012), national (Goward et al., 2015; Hermosilla et al., 2016), and global scales (Hansen et al., 2013). Reviews of these new developments have been provided by (Banskota et al., 2014; Gómez et al., 2016). Compared with disturbance products derived using temporally sparse observations, use of dense time series observations can improve the precision of the timing of mapped disturbance events and reduce omission errors that may arise when the spectral signal of a disturbance event fades quickly due to rapid post-disturbance recovery (Lunetta et al., 2004; Masek et al., 2008). Further, use of time series analysis methods together with machine learning or other analytical algorithms may also allow determining the type or causal agent of disturbance events (Hermosilla et al., 2015b; Kennedy et al., 2015; Moisen et al., 2016; Schroeder et al., 2011; Zhao et al., 2015).

While rapid progress has been made in determining the occurrence and causal agent of disturbance events, quantifying their intensity is more challenging (Schroeder et al., 2011). Although calculating the spectral signal of a disturbance event using pre- and post-disturbance observations is relatively straightforward, linking these spectral changes to measures of physical changes requires reference data on those physical changes. It has been demonstrated that given reference data, burn severity could be estimated based on normalized burn ratio or other measures of spectral changes or radiative transfer models (RTMs) (De Santis et al., 2009; Escuin et al., 2008; Soverel et al., 2010). In the Pacific Northwest region, Healey et al. (2006) showed that logging intensity as measured by basal area removal or canopy cover change was correlated with several measures of spectral changes. While reference data derivation for land cover studies is expensive and time consuming in general, deriving reference data on disturbance intensity is substantially more difficult, as determining the intensity of a disturbance event typically requires two measurements, one made before that event and the other after. This is exacerbated by the fact that under most circumstances only small fractions (1–2% or less) of the forests in a region are subject to measurable disturbances within a given time period (e.g., a year). Consequently, the chance of obtaining both pre- and post-disturbance measurements for an actual disturbance event using probability based sampling methods is low. Intensified sampling targeting disturbed areas could be allocated when the timing and location of certain disturbance events are known beforehand (e.g., planned harvest) so that resources (if available) can be allocated for collecting needed ground measurements before and after those events.

The Forest Inventory and Analysis (FIA) program of the US Forest Service has been continuously collecting one of the most valuable datasets for quantifying forest disturbance intensity using ground measurements. To meet its congressional mandate to provide routine assessment of the nation's forests, FIA has developed a large network of permanent plots distributed across the nation and sends field crew to measure these plots periodically (Smith, 2002). For plots that experienced disturbances, the intensity of those disturbances could be quantified using the field measurements made before and after those disturbances. The primary goal of this study is to develop an approach that integrate the FIA dataset with Landsat based disturbance products for annual mapping of forest disturbance intensity and use this approach to produce annual forest disturbance intensity maps for North and South Carolina. In the following sections, we first describe the data and methods and then present the derived results. A summary of the derived conclusions is provided after a discussion of the strength and limitations of this work and implications for future study.

2. Data and methods

2.1. Study area

The study area included the states of North and South Carolina, both of which had long histories of logging activities. South Carolina extends across the Piedmont (in the northwest) and Coastal Plain (in the southeast) physiographic provinces. More than two thirds (68.5% or 53,013.8 km^2) of South Carolina's land was forested in 2011 with 1.2% considered reserved or protected from commercial forestry (Rose, 2016). Of the 88% of South Carolina forest land in private ownership in 2011, only 2.9% (1359.7 km^2) was owned by industrial owners who are incorporated and own a primary wood processing mill. Loblolly-shortleaf pine group is the dominant forest group in South Carolina (42%) followed by Oak-Hickory (22.1%), and Oak-Gum-Cypress (15.3%).

North Carolina contains three main physiographic provinces moving from Mountain in the western border in Tennessee to Piedmont in the center of the state and finally Coastal Plain out towards the Atlantic coast. In 2007, 60% (75,199.3 km^2) of North Carolina's land base was forest land with only 2% reserved from commercial forestry (Brown et al., 2014). 88% of the states' industrial timberland (5665.5 km^2 in total) is located in the Coastal Province. Oak-Hickory is the dominant forest type on timberland at 40%, followed by Loblolly-shortleaf pine types (29%), Oak-pine (13%) and Oak-Gum-Cypress (10%). Province level species distributions vary and do not correspond to the state averages. For example, in the Coastal Plain province, Loblolly-shortleaf pine types are the dominant species type (> 40%). The study region is covered by 16 World Reference System 2 (WRS2) path/row tiles, including path 14–19/row 35–36, path 15–17/row 37, and path 16/row 38 (Fig. 1).

2.2. Approach overview

The overall methodology was built upon the progress in forest disturbance analysis using time series Landsat observations. It seeks to establish relationships between physical measures of disturbance intensity and Landsat disturbance products based on reference data derived using repeat measurements collected through the FIA program, and uses those relationships to convert spectral changes to disturbance intensity measures for each disturbance pixel. This was achieved through a processing flow that consisted of three major components: 1) generation of forest disturbance products, 2) reference data derivation, and 3) model development and map generation (Fig. 2). The required datasets are discussed in the following sections where details on each processing component are provided.

2.3. Production of disturbance and spectral change products

The disturbance products used in this study were generated through a recent phase of the North American Forest Dynamics (NAFD) study (Goward et al., 2008). A major goal of the NAFD study was to map forest disturbances annually from 1980s onward for the conterminous US (CONUS) using Landsat data (Zhao et al., 2018). The derived map products for the 1986–2010 period are distributed through a web portal of the Oak Ridge National Laboratory's Distributed Active Archive Center (Goward et al., 2015). These map products were generated using the vegetation change tracker (VCT) algorithm (Huang et al., 2010) and annual Landsat time series stack (LTSS), where each LTSS consisted of one clear view or near clear view image or image composite per year for each WRS2 path/row tile (Huang et al., 2009a). Details about the LTSS-VCT approach have been provided in several publications (Huang et al.,

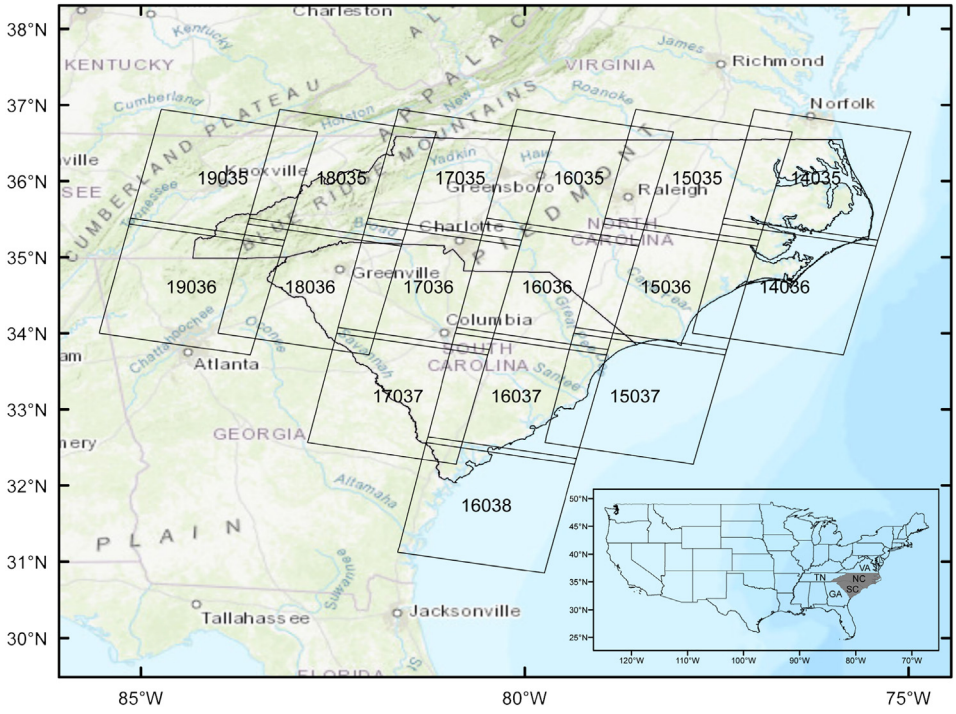

Fig. 1. Location of the study region and the Landsat path/row tiles covering the study region. The Landsat path/row tiles are in PP0RR format. Note that the coverage of some path/row tiles, such as 16036, spans both South and North Carolina.

2011; Huang et al., 2010; Huang et al., 2009b). Prior to its use to produce the CONUS-wide NAFD products, it was tested extensively across the US (Li et al., 2009a, 2009b), with many of the derived products having been validated (Huang et al., 2011; Thomas et al., 2011), including some located within the study region of this work (Huang et al., 2009b; Huang et al., 2015). For this study, the NAFD record over North and South Carolina was extended to 2015.

For each disturbance event mapped by VCT, the algorithm calculated a suite of spectral changes using several spectral indices, including the normalized difference vegetation index (NDVI) (Tucker, 1979), normalized burn ratio (NBR) (Miller and Thode, 2007), normalized difference moisture index (NDMI) (Jin and Sader, 2005), an integrated forest z-score (IFZ), and forest z-scores (FZ) calculated using Landsat bands 4 (B4FZ) and 5 (B5FZ) (Huang et al., 2010). These indices have been used in many vegetation, surface water, and disturbance studies (Jin and Sader, 2005; Wilson and Sader, 2002). They were defined as follows:

$$NDVI = \frac{B_4 - B_3}{B_4 + B_3} \quad (1)$$

$$NBR = \frac{B_4 - B_7}{B_4 + B_7} \quad (2)$$

$$NDMI = \frac{B_4 - B_5}{B_4 + B_5} \quad (3)$$

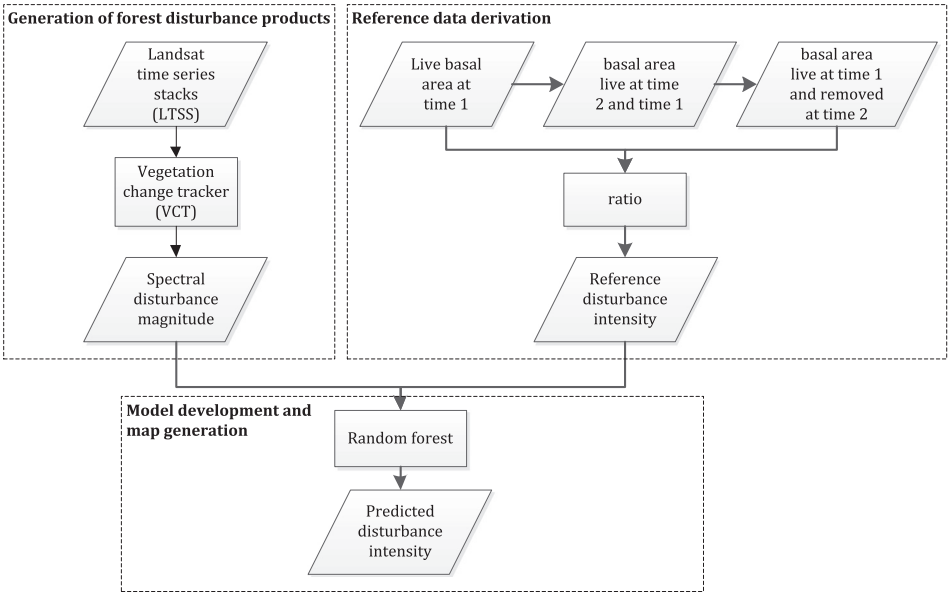

Fig. 2. Processing flow of the proposed approach for mapping forest disturbance intensity.

Table 1
Experiment design for estimating disturbance intensity from different groups of spectral disturbance magnitude data.

Scenario 1	Scenario 2	Scenario 3
Delta variables: $IFZ_2 - IFZ_1$, $NDVI_2 - NDVI_1$, $NBR_2 - NBR_1$, $B4FZ_2 - B4FZ_1$, $B5FZ_2 - B5FZ_1$	Normalized before/after ratio: $1 - IFZ_1 / IFZ_2$, $1 - NDVI_2 / NDVI_1$, $1 - NBR_2 / NBR_1$, $1 - NDMI_2 / NDMI_1$, $1 - B5FZ_1 / B5FZ_2$	Delta variables + Normalized before/after ratio

$$IFZ = \sqrt{\frac{1}{3}\sum_{band3,5,7}\left(\frac{B_i - \overline{B}_i}{SD_i}\right)^2} \quad (4)$$

$$B4FZ = \frac{B_4 - \overline{B}_4}{SD_4} \quad (5)$$

$$B5FZ = \frac{B_5 - \overline{B}_5}{SD_5} \quad (6)$$

where B_i is the reflectance value of a 30 m pixel in Landsat band i, and $\overline{B}_i$ and SD_i the mean and standard deviation of dark dense forest samples identified by VCT in each image. These indices were used to calculate absolute (delta variables) and relative (normalized before/after ratio, NBA ratio) spectral changes following the equations listed in Table 1, where the subscript value 1 and 2 refer to pre- and post-disturbance observations, respectively.

2.4. Reference data derivation

Reference disturbance intensity data were derived based on repeat measurements over FIA plot locations. The intensity of disturbance events and their impacts can be measured in different ways. The intensity of fire disturbances, for example, has been quantified using burn severity indices (Chen et al., 2011; Soverel et al., 2010) or heat release (Lentile et al., 2006). The intensity of weather/climate events could be measured by the strength of wind, amount of precipitation, or ice accumulation (Chambers et al., 2007; Peterson, 2007; Proulx and Greene, 2001). For logging, basal area or canopy cover removal has been used (Healey et al., 2006). Since logging is a dominant disturbance type in the study area, basal area removal was used in this study. It may be used to infer biomass and other structure changes as basal area has been used to calculate biomass and is directly related to other forest properties such as height and canopy cover (Gill et al., 2000; Jenkins et al., 2003)

FIA has over 125,000 Tier 2 plots distributed across contiguous U.S. with a nominal spacing of approximately 5 km (or 2500 ha) per plot (Smith, 2002). Those on forestland are visited periodically by field crews to collect ground measurements. Following the 1998 Farm Bill FIA adopted an annual inventory strategy that incorporated a nationally consistent, spatially and temporally balanced sampling design (Gillespie, 1999; Smith, 2002). In the eastern states, such as North and South Carolina, the Tier 2 plots are divided into 5 panels, each of which is remeasured in a year. This approach ensures that there is a constant rollout of remeasured plot data annually, and a full remeasurement cycle for all plots is completed in 5 years. By the time of this study, three full cycles of measurements collected following the annual inventory strategy were available in South Carolina (2006, 2011, and 2016) and two in North Carolina (2007 and 2012).

The two states have 3789 plots with unique geographic locations. Only those that had been measured at least twice since 1999 and were disturbed between those measurements could be used to calculate disturbance intensity. Pre-1999 FIA data were not used in this study as they might not be completely consistent with post-1999 measurements due to changes made to the inventory strategy following the 1998 Farm Bill. South Carolina had 152 plots that met these requirements and North Carolina had 264.

For each plot visited (some plots may not be sampled during a panel due to adverse conditions or denied access), FIA field crews measured diameter at-breast-height (dbh) for each tree located on the plot that had a dbh of at least 12.7 cm. Basal area was calculated from dbh directly. Each site tree record was identified using a unique sequence number. When a tree measured in a previous annual inventory was remeasured, the individual tree sequence number from both cycles were linked, making it possible to track the trees removed due to disturbance and hence the total basal area removed during a remeasurement cycle.

Following a definition used by (Healey et al., 2006), "disturbance intensity" was measured by percent basal area removal (PBAR), i.e., the amount of basal area removed by disturbance, normalized to the pre-disturbance value. Because trees over an FIA plot can grow substantially during the years between two consecutive FIA measurements, a simple difference between such measurements does not provide a direct measure of basal area removed by disturbances. It is the net change between basal area loss caused by disturbances and gain resulting from the growth of unremoved trees plus newly added trees that met the minimum measurement size requirement (i.e., dbh ≥ 12.7 cm) at time 2 but did not exist or were too small to measure at time 1.

To calculate basal area removal due to disturbances occurred between two FIA measurements, we tracked the individual trees that were measured at both time 1 and time 2 using the tree identification number. Those that existed at time 1 but not at time 2 were assumed to be removed by disturbances occurred between two measurements. Let $TBA1$ be the total basal area of all live trees measured at time 1 and $BA21$ the basal area of trees that existed at both time 1 and time 2 measured at time 1, then the basal area removal (BAR) caused by disturbances occurred immediately after the time 1 measurement is:

$$BAR = TBA1 - BA21 \quad (7)$$

BAR caused by a disturbance occurred one or more years after time 1 measurement likely will be different from that calculated using Eqs. (7), as the removed and unremoved trees likely will grow at different rates between time 1 and the occurrence of the disturbance. Given the limited amount of growth that can occur within such short temporal intervals (< 5 years in this study area), however, these differences should be small in general, and can be further reduced by normalizing Eq. (7) by the time 1 total basal area $TBA1$ to calculate the percent basal area removal ($PBAR$):

$$PBAR = \frac{TBA1 - BA21}{TBA1} \quad (8)$$

A flowchart of the procedure for calculating PBAR using remeasured FIA plot data is provided in Fig. 2.

2.5. Model development

With the above derived reference data, we explored the relationships between PBAR and spectral change measures listed in Table 1 in several ways. First, the ordinary least square linear regression method was used to examine relationships between PBAR and each individual spectral change measure. The Random Forest (RF) regression tree algorithm was then used to establish more robust models. RF has been used to derive land cover and other biophysical variables using remote sensing data in numerous studies (Belgiu and Drăguţ, 2016; Cutler et al., 2007). It is built as an ensemble of regression trees (Breiman, 2001), where each tree partitions the explanatory variables into a series of boxes that contain the most homogeneous collection of outcome possible. An RF tree is developed by selecting a small random sample of explanatory variables at the root node, based on which the best split is made. At each subsequent node, another small sample of explanatory

variables is chosen and the best split is made. The tree continues to grow until it reaches its largest possible size.

To assess the usefulness of different spectral change measures for PBAR modeling, three groups of RF models were evaluated. The first and second groups were developed using the delta and NBA ratio variables listed in Table 1, respectively, and the third was developed by combining the two variable types. These model groups were evaluated using a five-fold cross validation method. In this method, the reference samples were divided into five equal sized subsets in a random way. Four of those subsets were used to train the RF algorithm to build a model and the remaining subset was used to evaluate that model. This was repeated five times such that each subset was used to evaluate the model generated by the other four subsets. The results from all five experiments were pooled together to calculate the root mean square difference between the predicted values and the FIA data and the coefficient of determination (R^2) of their relationships as measures of model performance. The cross-validation results derived this way should be considered reasonably unbiased and equivalent to what could be derived using independent validation datasets, because in each of the five folds of the cross-validation, the test samples were selected randomly and had essentially no spatial autocorrelations with the training samples (Friedl et al., 1999; Huang et al., 2003).

2.6. Map products generation and assessment

Based on the cross-validation, the model that had the best performance was used to produce PBAR maps for all disturbances mapped by VCT. As discussed earlier, the cross-validation results for this model should provide a reasonably realistic assessment of these maps not biased by spatial autocorrelation, as the FIA plots used in model development and cross validation were located at least 5 km apart from each other and hence had minimal, if any, spatial autocorrelation. Further evaluation included comprehensive visual assessments of the mapped PBAR values against the input Landsat images. By the time of this study, Google Earth had two or more high resolution images in some areas within the study region. Those images were examined to provide visual verification of the derived PBAR maps. Finally, the validated PBAR maps were used to evaluate the distribution, spatial variability and temporal dynamics of disturbance intensity across the entire study region.

3. Results

3.1. Relationships between PBAR and spectral change variables

Relationships between PBAR and individual spectral change variables are weak (Fig. 3). 4 of the 10 variables listed in Table 1, including two delta variables and two normalized ratio variables, explained about 20% of the total PBAR variance of the selected FIA plots. The other 6 variables had weaker relationships with PBAR, suggesting that use of spectral changes from a single band or spectral index would not allow robust mapping of PBAR in North and South Carolina.

3.2. Effectiveness of PBAR modeling using multiple variables

Despite the weak relationships between PBAR and individual spectral change variables, the Random Forest algorithm allowed more robust modeling of PBAR when multiple variables were used, which is probably because of the contribution of combined information from multiple variables. The cross-validation assessment results revealed that the RF model developed using the five delta variables explained 67% of the total PBAR variance (Fig. 4(a)) while that developed using the normalized ratio variables explained 62% (Fig. 4(b)). Use of both variable types explained nearly 70% of the total PBAR variance (Fig. 4(c)). All three models over predicted towards the low end and under predicted towards the high end.

Since the RF model developed using both variable groups performed better than those developed using one group alone, that model was used to produce the final PBAR maps across the Carolinas at the native Landsat 30 m spatial resolution for all years from 1986 to 2015. The following were observed based on comprehensive visual assessments using the input Landsat images and high resolution satellite images available from Google Earth.

The spatial variations of mapped PBAR values within disturbance patches were confirmed by available post-disturbance high resolution Google Earth images. Visually identifiable cleared patches typically had high PBAR values. Landsat pixels with lower PBAR values often had some trees left that could be identified using post-disturbance high resolution images. Higher disturbance magnitudes are observed in the center of the disturbed patch, with a decreasing trend towards the edges. A further examination of the spatial pattern reveals that the boundary of a patch is often composed of both forest and nonforest, the heterogeneity of which causes a smaller value of disturbance intensity compared with that in the center of a patch. Some edge pixels of stand clearing patches also had low PBAR values because of the mixed pixels.

While most of the differences between predicted PBAR values and the reference data likely due to model errors, some of them could arise from differences between FIA measurement date and the acquisition date of Landsat image. Even when an FIA re-measurement and a disturbance event occurred in the same year, the field crew could visit before that disturbance event. Consequently, the FIA based PBAR would be much lower than the estimate derived using pre- and post-disturbance Landsat observations. The underestimation of high disturbance intensity, especially the underestimation of some stand clearing disturbance as partial disturbance, could be a result of the FIA plots located near the edge of the disturbed patches. The heterogeneity along the boundary of the disturbed patch could lead to large discrepancy between mapped and observed values if high and low intensity values are close to each other in the map. Because of the scale difference between FIA plots and Landsat pixels, the validation results at heterogeneous sites are expected to have a lower accuracy than those at homogenous sites (Tao et al., 2018; Tao et al., 2016; Tao et al., 2015; Tao et al., 2009; Xu et al., 2009).

3.3. Spatial-temporal patterns of disturbance intensity in the Carolinas

As expected, the PBAR maps revealed that forest disturbance intensity varied greatly across space and through time in the study region (Huang et al., 2015). Locally, most disturbance patches had variable PBAR values within each patch, although stand clearing events typically resulted in more homogenous patches with high PBAR values. A spatial-temporal synopsis map showing the PBAR values of disturbances during the period 1986–2015 revealed that across the region, high intensity disturbances occurred mostly in the Middle Atlantic Coastal Plain, Southeastern Plains, and Piedmont ecoregions, while the Southern Coastal Plain ecoregion had lower disturbances in general (Fig. 5). Home to the Great Smoky Mountains National Park and several national forests, the Blue Ridge ecoregion was dominated by mid to low intensity disturbances. The relative proportions of disturbances that had high PBAR values (e.g., > 65%) were lower in North Carolina than those in South Carolina in Fig. 6. This was largely due to the dominance of low PBAR values in the Blue Ridge ecoregion, which was mostly located within North Carolina in the study region (Fig. 5). In the Piedmont and Southeastern Plains ecoregions, North Carolina appeared to have more mid to low intensity disturbances than South Carolina.

PBAR had multi-modal distributions that differed substantially from year to year. The histogram of the 2007 PBAR map, for example, had one major peak and two minor years (Fig. 7(b)).while the 1995 histogram had two major peaks (Fig. 7(a)) and the 2009 histogram three (Fig. 7(c)). Over the 30-year observing period, the PBAR values as represented by the spatial-temporal synopsis map shown in Fig. 6 had a distribution skewed towards the high end with two obvious peak

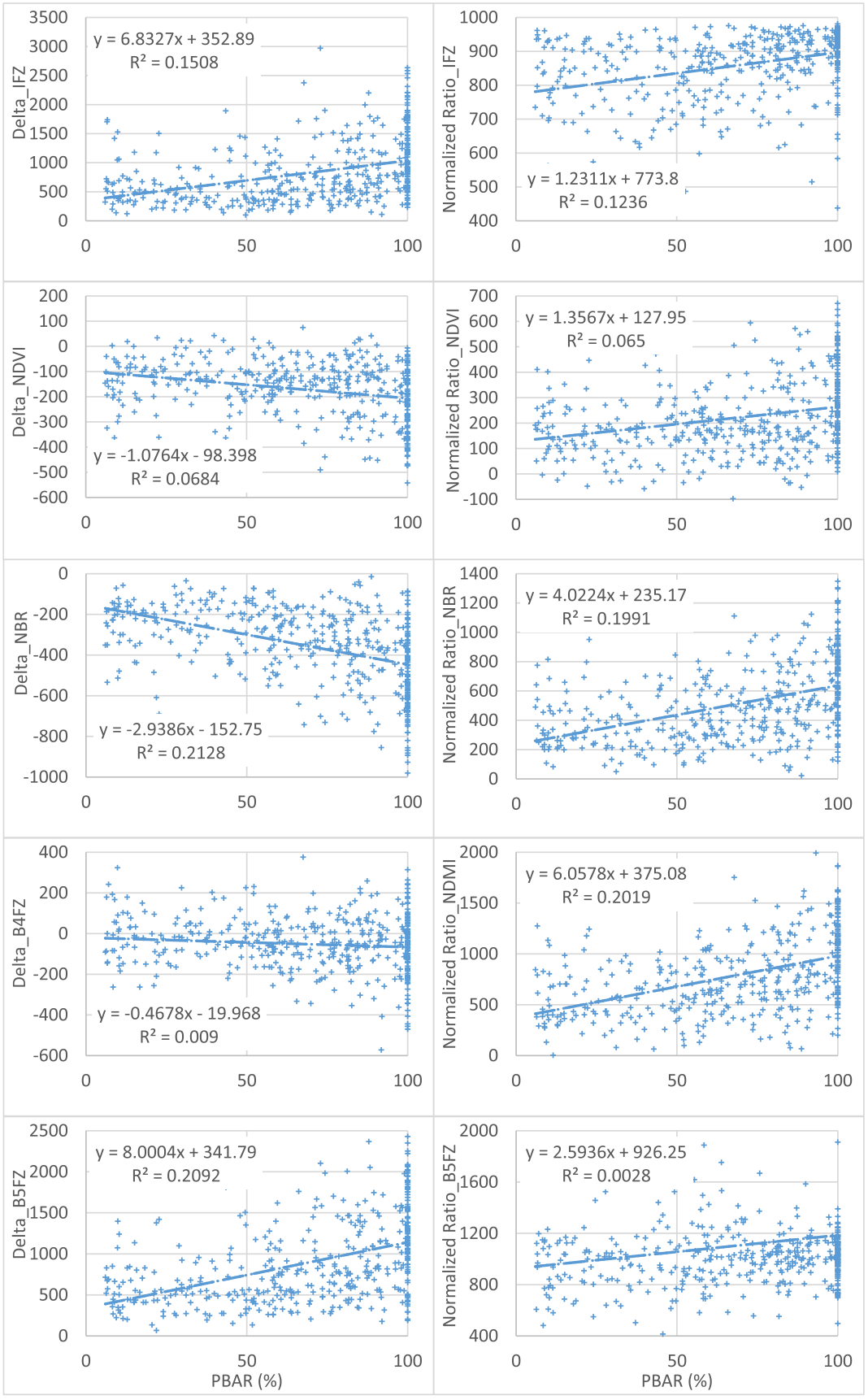

Fig. 3. Relationships between PBAR and individual spectral change variables.

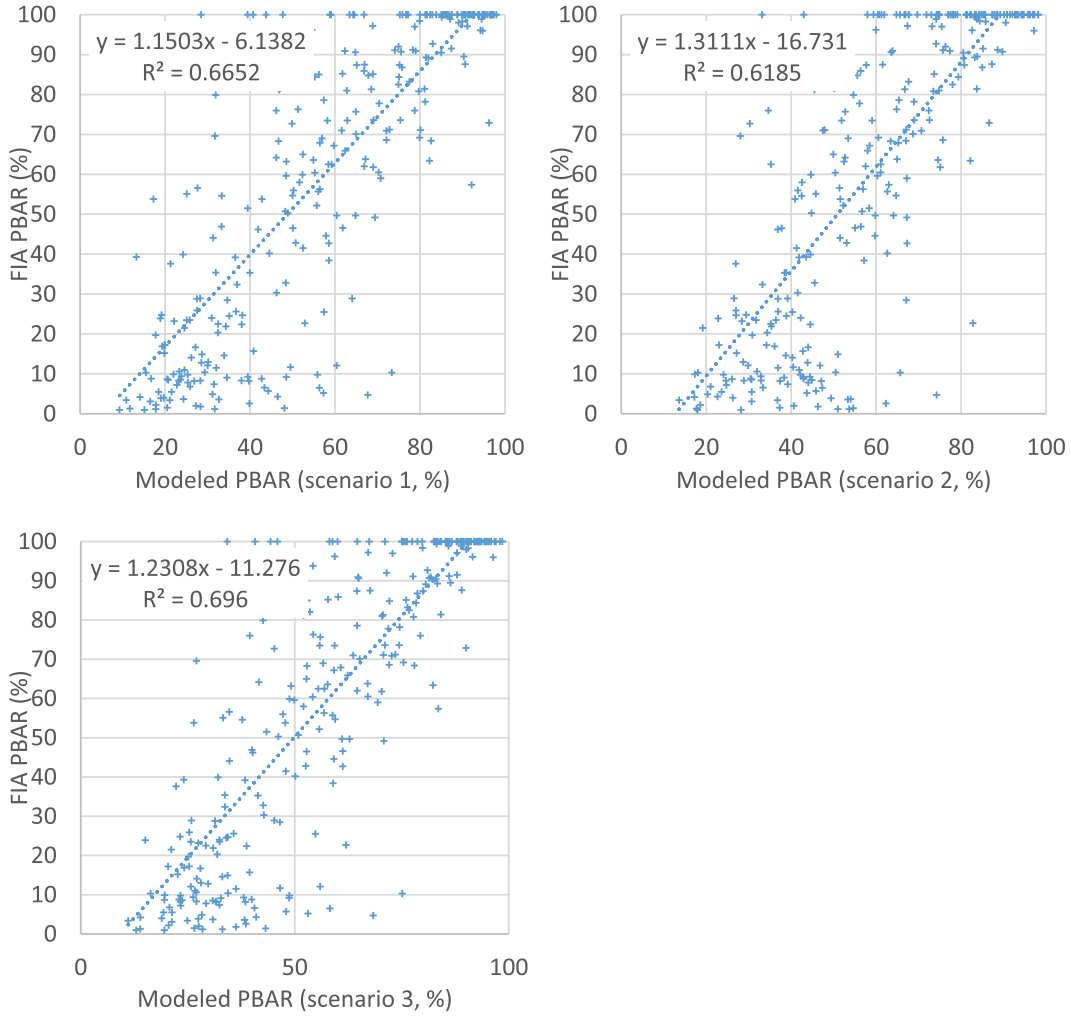

Fig. 4. Scatterplots between the modeled disturbance intensity and the FIA data in North Carolina using training data of delta variables in Scenario 1, normalized before/after radio in Scenario 2, or a combination in Scenario 3.

located between 80% and 100% and two less obvious ones centered around 60% and 40% (Fig. 7(d)). PBAR histograms of the two states had similar peaks, but their relative magnitudes were different between the two states.

The derived PBAR maps allowed calculation of disturbance area at different intensity levels. Following the FIA's use of an 80% basal area removal threshold to separate clearcutting harvest from partial harvest (Birdsey and Lewis, 2003), the time series maps revealed that only about a quarter of the disturbances in the Carolinas as mapped using the presented LTSS-VCT approach were clearcutting. The average annual disturbance areas for clearcutting and partial disturbance events were 1143 km^2 and 3287 km^2, respectively (Fig. 8). The total area subject to clearcutting was relatively stable over time, but that for partial disturbances had substantial interannual variability, fluctuating between 1919 km^2 and 6000 km^2. Some of the large increases in disturbance area were associated with severe damages caused by hurricanes and other tropical storms that often passed through the Carolinas or made landfall in the coastal areas (Huang et al., 2015). Some were associated with human activities, such as urbanization and logging. We also observed a lot of selective logging activities, which is an effective way for forest management.

4. Discussion

The impact of a disturbance event is largely determined by its intensity. A stand-clearing event could result in large changes in surface properties such as roughness and albedo and near complete transfer of carbon from the standing biomass pool to other carbon pools, whereas the impact of a partial canopy removal event could be much smaller. When a forest stand is cleared, its age is reset to 0, but if only a fraction of trees in the stand are removed, the remaining trees determine its age. While great progress has been made in mapping forest disturbances at scales ranging from local to global, determining the intensity of mapped disturbance events is more challenging. This study demonstrates an approach designed to address this challenge. It builds on the VCT algorithm to map forest disturbances using annual Landsat time series and relies on field inventory data to derive reference data. The derived results revealed large spatial-temporal variations in forest disturbance intensity, which would likely cause large uncertainties if not considered in assessing the impact of forest disturbances.

In the states of North and South Carolina, PBAR values derived using this approach explained about two thirds of the variance of PBAR values calculated using FIA plot data. Further improvements might be achievable through integrated use of spectral and spatial information (Wulder, 1998). While synthetic aperture radar (SAR) measurements have saturation problems for forest monitoring, which is wavelength dependent (Balzter, 2001; Lucas et al., 2004), they are generally more sensitive to forest structure than optical data, and hence can be used to improve the characterization of disturbance intensity. Now that the Sentinel-1 constellation is already in orbit providing systematic acquisition of time series SAR images across the globe, and more SAR systems with similar or better capabilities are being developed, integrated use of

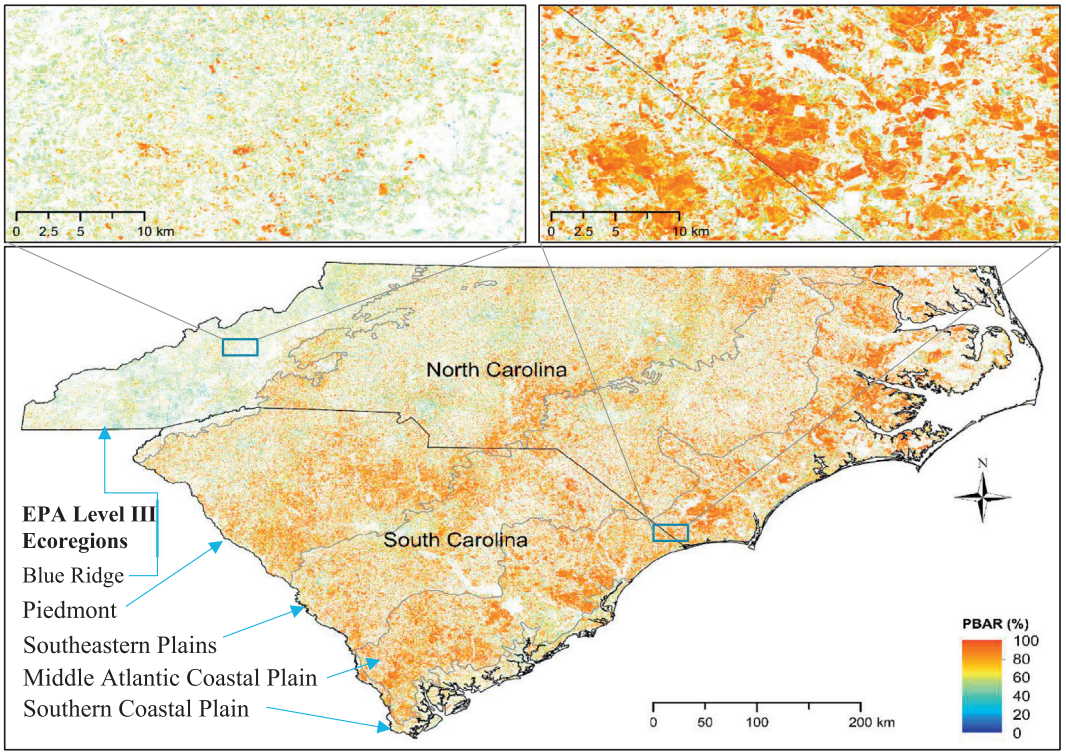

Fig. 5. Temporal integrated PBAR map (only the highest value is depicted if a pixel had more than one disturbance over the 30-year observing period) showing the general patterns of disturbance intensity over the Carolinas.

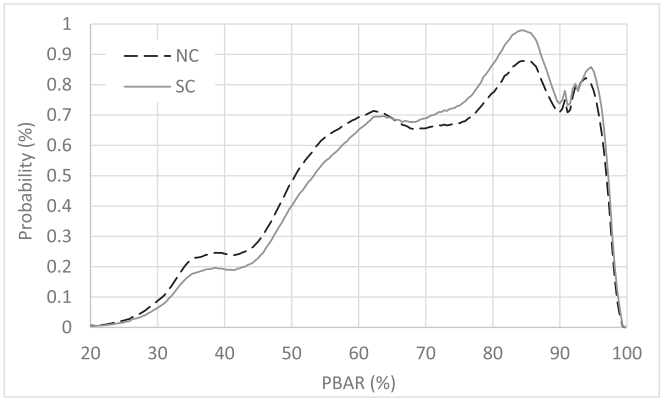

Fig. 6. Histogram of disturbance intensity in North Carolina and South Carolina.

optical and SAR time series to improve the characterization of disturbance intensity and other key attributes of vegetation dynamics will become increasingly more feasible.

Better spatial-temporal match between the reference data and Landsat observations could also help. Given the large geographic area of the two states and the 30-year span of this study, there is no doubt that the FIA data is by far the best for deriving the reference PBAR data needed by this study. However, the spatial coverage of an FIA plot may not match that of the closest 30-m Landsat pixel. An FIA plot consists of four equal-sized circular subplots covering a total area of 672.5 m^2. These subplots are arranged such that they represent an area with a radius of about 44 m or larger. Since the spatial coverage of a Landsat pixel may not match that of an FIA plot or subplot exactly, the validation results are generally better in relatively homogenous sites.

Temporal mismatch between FIA data and Landsat observations could also introduce errors. For example, when an FIA remeasurement is available in the same year as a disturbance detected by the VCT algorithm over a plot location, by algorithm design the Landsat image used in that year were acquired after the occurrence of the disturbance. But the FIA crew might visit that plot before the occurrence, or for a gradual process that took weeks or longer to complete, during the early stage of the disturbance event. Consequently, the plot should have a predicted PBAR value that matches the intensity of the disturbance event at the time when the Landsat image was acquired, but the value from the FIA data could be near 0. Further, the 5-year remeasurement interval of the FIA data might introduce uncertainties in determining the PBAR value for a disturbance occurred in a specific year, especially for plots that had multiple disturbance within the 5-year period. Such temporal mismatches could cause problems for model development and validation. When a plot with temporal mismatch problem is used as a validation point, it will inflate the error estimate. When it is used as part of the training data, it constitutes an error in the training data, and hence could affect model performance.

Despite the limitations discussed above, the successful use of this approach to quantify forest disturbance intensity as measured by percent basal area removal for the entire North and South Carolina over a 30-year period spanning from 1985 to 2015 is a demonstration of its robustness over large study regions where both Landsat time series observations and FIA-like inventory data exist. Annual Landsat observations have been available since 2000 across the globe and much earlier for many regions (Goward et al., 2006; Wulder et al., 2016). FIA-like forest inventory data have been collected across CONUS and in many other countries. While FIA-like inventory data are typically not publicly available, they could be reached through special agreements among relevant parties. Therefore, the approach developed through this study could be used to generate forest disturbance products for other regions of CONUS as well as countries with at least one set of FIA-like repeat measurements.

To improve the robustness of model development and product validation in such studies, it may be necessary to collect more ground-based reference data in addition to available inventory data. Because determining the intensity of a disturbance event requires at least two

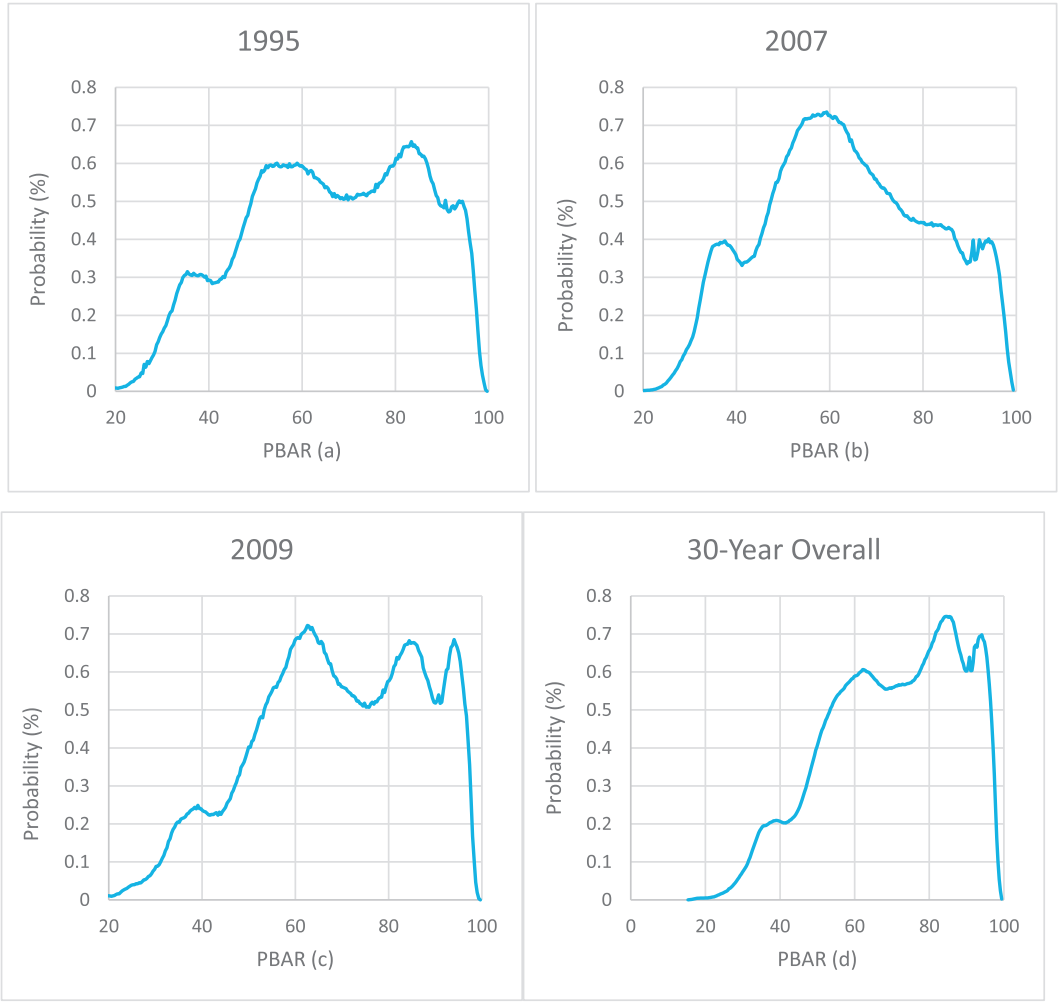

Fig. 7. Histograms of disturbance intensity in 1995, 2007, 2009, and 30-year overall.

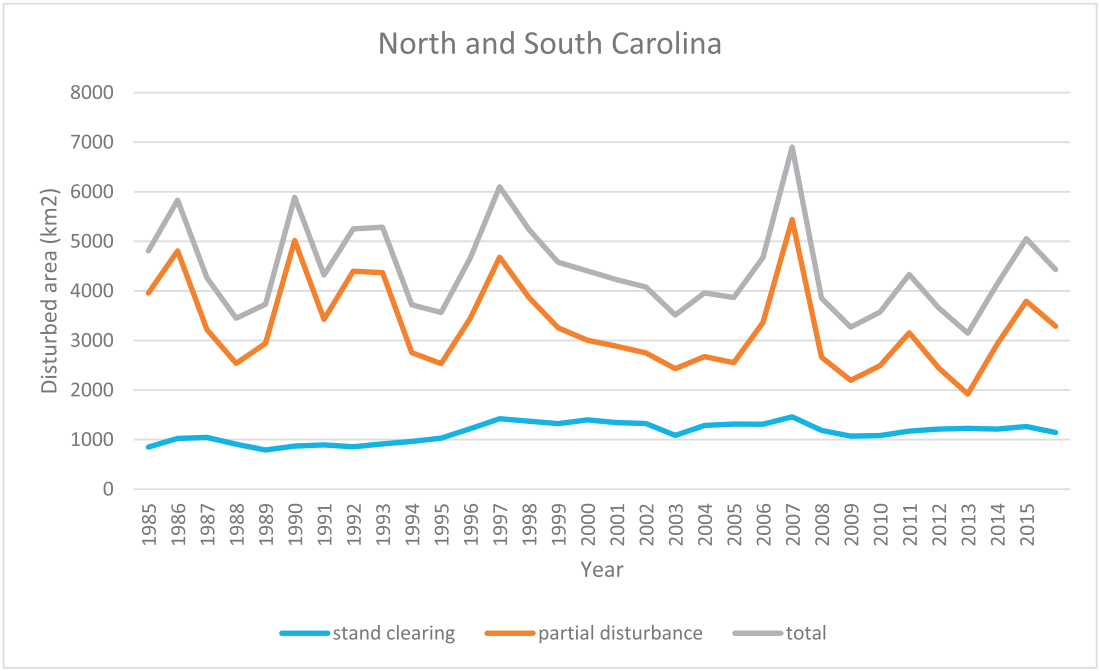

Fig. 8. Areas of stand clearing, partial disturbance, and the total over time.

measurements, one made before that event and the other after, in most regions there are far fewer samples that can provide information on disturbance intensity than on the status of forest at a specific time point. In the Carolinas, only 416 of the 3789 plots with unique geographic locations had valid information on disturbance intensity. Such a small number of reference samples limited our ability to use a portion (e.g., 40%) of the dataset to provide an independent assessment of a final model trained using the remaining samples, because doing so might result in an inadequately trained model due to insufficient training samples or unrepresentative validation results due to insufficient test samples, or both. Therefore, accuracy estimates derived through such an independent assessment might be unrepresentative of the final products produced in this study.

Given the fact that under most circumstances only small fractions (1–2% or less) of forests in a region are subject to measurable disturbances within a given time period (e.g., a year), the chance of obtaining both pre- and post-disturbance measurements for an actual disturbance event using probability-based sampling methods is low. Intensified sampling targeting disturbed areas will be needed to increase the amount of reference data on disturbance intensity. Given available resources, this could be achieved through well-coordinated field campaigns for cases when the timing and location of certain disturbance events (e.g., planned harvest) are known before the occurrence of the events. For natural disturbances whose occurrences are often unknown beforehand, conducting fieldwork immediately after those events over areas that had pre-event measurements will be highly valuable.

5. Conclusions

The disturbance intensity could be predicted from spectral disturbance magnitude with an uncertainty of 14% in North Carolina. Overall, the R^2 between the predicted disturbance intensity and the reference data is around 0.66. Results show that the relative proportions of disturbances that had high PBAR values were lower in North Carolina than those in South Carolina. This was largely due to the dominance of low PBAR values in the Blue Ridge ecoregion, which was mostly located within North Carolina in the study region. The area of stand clearing disturbances remains relatively stable around 1143 $km^2\,yr^{-1}$ in North and South Carolina throughout the period of observations (1985–2015). The average amount of forest area affected by partial disturbance is much higher at 3287 $km^2\,yr^{-1}$. The area of partial disturbances has strong inter-annual variability with a high value of 6000 km^2 in 2007 and a low value of 1919 km^2 in 2013. Due to the dominance of partial disturbance, the total disturbance area has similar pattern as partial disturbance area in the two regions. Future work could be integrated use of optical and SAR time series and collection of more ground-based reference data through intensified sampling targeting disturbed areas to improve the characterization of disturbance intensity.

Acknowledgements

The authors thank Dr. Samuel Goward for thoughtful comments on some figures. We are thankful to the NASA LEDAPS project team members for the atmospheric correction preprocessing code. This study contributes to the North American Carbon Program, with grant support from NASA's Land Cover and Land Use Change, Terrestrial Ecology, Carbon Cycle Science, and Applied Sciences Programs. Additional support was provided by the U.S. Geological Survey and USDA Forest Service. We thank Elizabeth Burrill for assisting with access to the FIA plot data, which was made possible through an MOU with the FIA program. The authors would like to thank the anonymous reviewers for their helpful comments and suggestions on the manuscript.

References

Balzter, H., 2001. Forest mapping and monitoring with interferometric synthetic aperture radar (InSAR). Prog. Phys. Geogr. 25, 159–177.
Banskota, A., Kayastha, N., Falkowski, M.J., Wulder, M.A., Froese, R.E., White, J.C., 2014. Forest monitoring using Landsat time series data: a review. Can. J. Remote. Sens. 40, 362–384.
Bari, M.A., Smettem, K.R.J., 2006. A conceptual model of daily water balance following partial clearing from forest to pasture. Hydrol. Earth Syst. Sci. 10, 321–337.
Belgiu, M., Drăguţ, L., 2016. Random forest in remote sensing: a review of applications and future directions. ISPRS J. Photogramm. Remote Sens. 114, 24–31.
Bengtsson, J., Nilsson, S.G., Franc, A., Menozzi, P., 2000. Biodiversity, disturbances, ecosystem function and management of European forests. For. Ecol. Manag. 132, 39–50.
Birdsey, R.A., Lewis, G.M., 2003. Current and historical trends in use, management, and disturbance of U.S. forestlands. In: Kimble, J.M., Heath, L.S., Birdsey, R.A., Lal, R. (Eds.), The Potential of U.S. Forest Soils to Sequester Carbon and Mitigate the Greenhouse Effect. CRC Press, New York, pp. 15–33.
Bonan, G.B., 2008. Forests and climate change: forcings, feedbacks, and the climate benefits of forests. Science 320, 1444–1449.
Breiman, L., 2001. Random forests. Mach. Learn. 45, 5–32.
Brown, M.J., New, B.D., Johnson, T.G., Chamberlain, J.L., 2014. North Carolina's forests, 2007. Asheville, NC: USDA-Forest Service, Southern Research Station. Resour. Bull. 112 (SRS-RB-199).
Burton, P.J., Parisien, M.A., Hicke, J.A., Hall, R.J., Freeburn, J.T., 2008. Large fires as agents of ecological diversity in the North American boreal forest. Int. J. Wildland Fire 17, 754–767.
Chambers, J.Q., Fisher, J.I., Zeng, H., Chapman, E.L., Baker, D.B., Hurtt, G.C., 2007. Hurricane Katrina's carbon footprint on U.S. Gulf Coast Forests. Science 318, 1107.
Chen, X., Vogelmann, J., Rollins, M., Ohlen, D., Key, C.H., Yang, L., Huang, C., Shi, H., 2011. Detecting post-fire burn severity and vegetation recovery using multi-temporal remote sensing spectral indices and field collected Composite Burn Index data in a mixed burn severity ponderosa pine forest. Int. J. Remote Sens. 32, 7905–7927.
Coppin, P., Lambin, E., Jonckheere, I., Nackaerts, K., Muys, B., 2004. Digital change detection methods in ecosystem monitoring: a review. Int. J. Remote Sens. 25, 1565–1596.
Cutler, D.R., Edwards, T.C., Beard, K.H., Cutler, A., Hess, K.T., Gibson, J., Lawler, J.J., 2007. Random forests for classification in ecology. Ecology 88, 2783–2792.
De Santis, A., Chuvieco, E., Vaughan, P.J., 2009. Short-term assessment of burn severity using the inversion of PROSPECT and GeoSail models. Remote Sens. Environ. 113, 126–136.
Devries, B., Verbesselt, J., Kooistra, L., Herold, M., 2015. Robust monitoring of small-scale forest disturbances in a tropical montane forest using Landsat time series. Remote Sens. Environ. 161, 107–121.
Escuin, S., Navarro, R., Fernandez, P., 2008. Fire severity assessment by using NBR (Normalized Burn Ratio) and NDVI (Normalized Difference Vegetation Index) derived from LANDSAT TM/ETM images. Int. J. Remote Sens. 29, 1053–1073.
Friedl, M.A., Brodley, C.E., Strahler, A.H., 1999. Maximizing land cover classification accuracies produced by decision trees at continental to global scales. IEEE Trans. Geosci. Remote Sens. 37, 969–977.
Frolking, S., Palace, M.W., Clark, D.B., Chambers, J.Q., Shugart, H.H., Hurtt, G.C., 2009. Forest disturbance and recovery: a general review in the context of spaceborne remote sensing of impacts on aboveground biomass and canopy structure. J. Geophys. Res. Biogeosci. 114.
Gill, S.J., Biging, G.S., Murphy, E.C., 2000. Modeling conifer tree crown radius and estimating canopy cover. For. Ecol. Manag. 126, 405–416.
Gillespie, A.J.R., 1999. Rationale for a National Annual Forest Inventory program. J. For. 97, 16–20.
Goetz, S.J., Bond-Lamberty, B., Law, B.E., Hicke, J.A., Huang, C., Houghton, R.A., McNulty, S., O'Halloran, T., Harmon, M., Meddens, A.J.H., Pfeifer, E.M., Mildrexler, D., Kasischke, E.S., 2012. Observations and assessment of forest carbon dynamics following disturbance in North America. J. Geophys. Res. Biogeosci. 117, G02022.
Gómez, C., White, J.C., Wulder, M.A., 2016. Optical remotely sensed time series data for land cover classification: a review. ISPRS J. Photogramm. Remote Sens. 116, 55–72.
Goward, S., Arvidson, T., Williams, D., Faundeen, J., Irons, J., Franks, S., 2006. Historical record of Landsat global coverage: Mission operations, NSLRSDA, and international cooperator stations. Photogramm. Eng. Remote. Sens. 72, 1155–1169.
Goward, S.N., Masek, J.G., Cohen, W., Moisen, G., Collatz, G.J., Healey, S., Houghton, R., Huang, C., Kennedy, R., Law, B., Turner, D., Powell, S., Wulder, M., 2008. Forest disturbance and North American carbon flux. EOS Trans. Am. Geophys. Union 89, 105–106.
Goward, S.N., Huang, C., Zhao, F., Schleeweis, K., Rishmawi, K., Lindsey, M., Dungan, J.L., Michaelis, A., 2015. In: U.o.M.-N. NEX (Ed.), NACP NAFD Project: Forest Disturbance History From Landsat, 1986–2010. ORNL DAAC, Oak Ridge, Tennessee, USA. http://daac.ornl.gov/cgi-bin/dsviewer.pl?ds_id=1290.
Hansen, M.C., Potapov, P.V., Moore, R., Hancher, M., Turubanova, S.A., Tyukavina, A., Thau, D., Stehman, S.V., Goetz, S.J., Loveland, T.R., Kommareddy, A., Egorov, A., Chini, L., Justice, C.O., Townshend, J.R.G., 2013. High-resolution global maps of 21st-century forest cover change. Science 342, 850–853.
Healey, S.P., Yang, Z., Cohen, W.B., Pierce, D.J., 2006. Application of two regression-based methods to estimate the effects of partial harvest on forest structure using Landsat data. Remote Sens. Environ. 101, 115–126.
Healey, S.P., Cohen, W.B., Yang, Z.Q., Brewer, C.K., Brooks, E.B., Gorelick, N., Hernandez, A.J., Huang, C.Q., Hughes, M.J., Kennedy, R.E., Loveland, T.R., Moisen, G.G., Schroeder, T.A., Stehman, S.V., Vogelmann, J.E., Woodcock, C.E., Yang, L.M.,

Zhu, Z., 2018. Mapping forest change using stacked generalization: an ensemble approach. Remote Sens. Environ. 204, 717–728.
Hermosilla, T., Wulder, M.A., White, J.C., Coops, N.C., Hobart, G.W., 2015a. An integrated Landsat time series protocol for change detection and generation of annual gap-free surface reflectance composites. Remote Sens. Environ. 158, 220–234.
Hermosilla, T., Wulder, M.A., White, J.C., Coops, N.C., Hobart, G.W., 2015b. Regional detection, characterization, and attribution of annual forest change from 1984 to 2012 using Landsat-derived time-series metrics. Remote Sens. Environ. 170, 121–132.
Hermosilla, T., Wulder, M.A., White, J.C., Coops, N.C., Hobart, G.W., Campbell, L.B., 2016. Mass data processing of time series Landsat imagery: pixels to data products for forest monitoring. Int. J. Digital Earth 9, 1035–1054.
Houghton, R.A., House, J.I., Pongratz, J., van der Werf, G.R., DeFries, R.S., Hansen, M.C., Le Quere, C., Ramankutty, N., 2012. Carbon emissions from land use and land-cover change. Biogeosciences 9, 5125–5142.
Huang, C., Homer, C., Yang, L., 2003. Regional forest land cover characterization using medium spatial resolution satellite data. In: Wulder, M., Franklin, S. (Eds.), Methods and Applications for Remote Sensing of Forests: Concepts and Case Studies. Kluwer Academic Publishers, Boston, pp. 389–410.
Huang, C.Q., Goward, S.N., Masek, J.G., Gao, F., Vermote, E.F., Thomas, N., Schleeweis, K., Kennedy, R.E., Zhu, Z.L., Eidenshink, J.C., Townshend, J.R.G., 2009a. Development of time series stacks of Landsat images for reconstructing forest disturbance history. Int. J. Digital Earth 2, 195–218.
Huang, C.Q., Goward, S.N., Schleeweis, K., Thomas, N., Masek, J.G., Zhu, Z.L., 2009b. Dynamics of national forests assessed using the Landsat record: case studies in eastern United States. Remote Sens. Environ. 113, 1430–1442.
Huang, C.Q., Kim, S., Song, K., Townshend, J.R.G., Davis, P., Altstatt, A., Rodas, O., Yanosky, A., Clay, R., Tucker, C.J., Musinsky, J., 2009c. Assessment of Paraguay's forest cover change using Landsat observations. Glob. Planet. Chang. 67, 1–12.
Huang, C.Q., Goward, S.N., Masek, J.G., Thomas, N., Zhu, Z.L., Vogelmann, J.E., 2010. An automated approach for reconstructing recent forest disturbance history using dense Landsat time series stacks. Remote Sens. Environ. 114, 183–198.
Huang, C., Schleeweis, K., Thomas, N., Goward, S., 2011. Forest dynamics within and around the Olympic National Park assessed using time series Landsat observations. In: Wang, Y. (Ed.), Remote Sensing of Protected Lands. Taylor & Francis, London, pp. 71–93.
Huang, C.Q., Ling, P.Y., Zhu, Z.L., 2015. North Carolina's forest disturbance and timber production assessed using time series Landsat observations. Int. J. Digital Earth 8, 947–969.
Hussain, M., Chen, D., Cheng, A., Wei, H., Stanley, D., 2013. Change detection from remotely sensed images: from pixel-based to object-based approaches. ISPRS J. Photogramm. Remote Sens. 80, 91–106.
Jenkins, J.C., Chomnacky, D.C., Heath, L.S., Birdsey, R.A., 2003. National scale biomass estimators for United States tree species. For. Sci. 49, 12–35.
Jin, S.M., Sader, S.A., 2005. Comparison of time series tasseled cap wetness and the normalized difference moisture index in detecting forest disturbances. Remote Sens. Environ. 94, 364–372.
Kennedy, R.E., Yang, Z.G., Cohen, W.B., 2010. Detecting trends in forest disturbance and recovery using yearly Landsat time series: 1. LandTrendr - temporal segmentation algorithms. Remote Sens. Environ. 114, 2897–2910.
Kennedy, R.E., Yang, Z., Cohen, W.B., Pfaff, E., Braaten, J., Nelson, P., 2012. Spatial and temporal patterns of forest disturbance and regrowth within the area of the northwest forest plan. Remote Sens. Environ. 122, 117–133.
Kennedy, R.E., Andrefouet, S., Cohen, W.B., Gomez, C., Griffiths, P., Hais, M., Healey, S.P., Helmer, E.H., Hostert, P., Lyons, M.B., Meigs, G.W., Pflugmacher, D., Phinn, S.R., Powell, S.L., Scarth, P., Sen, S., Schroeder, T.A., Schneider, A., Sonnenschein, R., Vogelmann, J.E., Wulder, M.A., Zhu, Z., 2014. Bringing an ecological view of change to Landsat-based remote sensing. Front. Ecol. Environ. 12, 339–346.
Kennedy, R.E., Yang, Z., Braaten, J., Copass, C., Antonova, N., Jordan, C., Nelson, P., 2015. Attribution of disturbance change agent from Landsat time-series in support of habitat monitoring in the Puget Sound region, USA. Remote Sens. Environ. 166, 271–285.
Kim, D.-H., Sexton, J.O., Noojipady, P., Huang, C., Anand, A., Channan, S., Feng, M., Townshend, J.R., 2014. Global, Landsat-based forest-cover change from 1990 to 2000. Remote Sens. Environ. 155, 178–193.
Lentile, L.B., Holden, Z.A., Smith, A.M.S., Falkowski, M.J., Hudak, A.T., Morgan, P., Lewis, S.A., Gessler, P.E., Benson, N.C., 2006. Remote sensing techniques to assess active fire characteristics and post-fire effects. Int. J. Wildland Fire 15, 319–345.
Li, M., Huang, C., Zhu, Z., Shi, H., Lu, H., Peng, S., 2009a. Assessing rates of forest change and fragmentation in Alabama, USA, using the vegetation change tracker model. For. Ecol. Manag. 257, 1480–1488.
Li, M., Huang, C., Zhu, Z., Shi, H., Lu, H., Peng, S., 2009b. Use of remote sensing coupled with a vegetation change tracker model to assess rates of forest change and fragmentation in Mississippi, USA. Int. J. Remote Sens. 30, 6559–6574.
Ling, P.Y., Baiocchi, G., Huang, C.Q., 2016. Estimating annual influx of carbon to harvested wood products linked to forest management activities using remote sensing. Clim. Chang. 134, 45–58.
Lu, D., Mausel, P., Brondizio, E., Moran, E., 2004. Change detection techniques. Int. J. Remote Sens. 25, 2365–2407.
Lucas, R.M., Moghaddam, M., Cronin, N., 2004. Microwave scattering from mixed-species forests, Queensland, Australia. IEEE Trans. Geosci. Remote Sens. 42, 2142–2159.
Lunetta, R.S., Johnson, D.M., Lyon, J.G., Crotwell, J., 2004. Impacts of imagery temporal frequency on land-cover change detection monitoring. Remote Sens. Environ. 89, 444–454.
Masek, J.G., Huang, C., Wolfe, R.E., Cohen, W., Hall, F., Kutler, J., Nelson, P., 2008. North American forest disturbance mapped from a decadal Landsat record. Remote Sens. Environ. 112, 2914–2926.
Masek, J.G., Cohen, W.B., Leckie, D., Wulder, M.A., Vargas, R., de Jong, B., Healey, S., Law, B., Birdsey, R., Houghton, R.A., Mildrexler, D., Goward, S., Smith, W.B., 2011. Recent rates of forest harvest and conversion in North America. J. Geophys. Res. Biogeosci. 116.
Meng, R., Dennison, P.E., Huang, C., Moritz, M.A., D'Antonio, C., 2015. Effects of fire severity and post-fire climate on short-term vegetation recovery of mixed-conifer and red fir forests in the Sierra Nevada Mountains of California. Remote Sens. Environ. 171, 311–325.
Miller, J.D., Thode, A.E., 2007. Quantifying burn severity in a heterogeneous landscape with a relative version of the delta Normalized Burn Ratio (dNBR). Remote Sens. Environ. 109, 66–80.
Moisen, G.G., Meyer, M.C., Schroeder, T.A., Liao, X., Schleeweis, K.G., Freeman, E.A., Toney, C., 2016. Shape selection in Landsat time series: a tool for monitoring forest dynamics. Glob. Chang. Biol. 22, 3518–3528.
Myers, N., 1997. The world's forests and their ecosystem services. In: Daily, G. (Ed.), Nature's Services: Societal Dependence on Natural Ecosystems. Island Press, Washington, DC, pp. 215–232.
Patterson, T.M., Coelho, D.L., 2009. Ecosystem services: foundations, opportunities, and challenges for the forest products sector. For. Ecol. Manag. 257, 1637–1646.
Peterson, C.J., 2007. Consistent influence of tree diameter and species on damage in nine eastern North America tornado blowdowns. For. Ecol. Manag. 250, 96–108.
Petranka, J.W., Eldridge, M.E., Haley, K.E., 1993. Effects of timber harvesting on southern Appalachian salamanders. Conserv. Biol. 7, 363–377.
Proulx, O.J., Greene, D.F., 2001. The relationship between ice thickness and northern hardwood tree damage during ice storms. Can. J. For. Res. 31, 1758–1767.
Rose, A.K., 2016. South Carolina's forests, 2011. Asheville, NC: U.S. Department of Agriculture Forest Service, Southern Research Station. Resour. Bull. 71 (SRS-208).
Schmidt, M., Lucas, R., Bunting, P., Verbesselt, J., Armston, J., 2015. Multi-resolution time series imagery for forest disturbance and regrowth monitoring in Queensland, Australia. Remote Sens. Environ. 158, 156–168.
Schofield, N.J., Ruprecht, J.K., 1989. Regional-analysis of stream salinization in southwest Western Australia. J. Hydrol. 112, 19 (&).
Schroeder, T.A., Wulder, M.A., Healey, S.P., Moisen, G.G., 2011. Mapping wildfire and clearcut harvest disturbances in boreal forests with Landsat time series data. Remote Sens. Environ. 115, 1421–1433.
Senf, C., Pflugmacher, D., Wulder, M.A., Hostert, P., 2015. Characterizing spectral-temporal patterns of defoliator and bark beetle disturbances using Landsat time series. Remote Sens. Environ. 170, 166–177.
Senf, C., Pflugmacher, D., Hostert, P., Seidl, R., 2017. Using Landsat time series for characterizing forest disturbance dynamics in the coupled human and natural systems of Central Europe. ISPRS J. Photogramm. Remote Sens. 130, 453–463.
Sexton, J.O., Noojipady, P., Anand, A., Song, X.-P., McMahon, S., Huang, C., Feng, M., Channan, S., Townshend, J.R., 2015. A model for the propagation of uncertainty from continuous estimates of tree cover to categorical forest cover and change. Remote Sens. Environ. 156, 418–425.
Singh, A., 1989. Digital change detection techniques using remotely-sensed data. Int. J. Remote Sens. 10, 989–1003.
Slade, E.M., Mann, D.J., Lewis, O.T., 2011. Biodiversity and ecosystem function of tropical forest dung beetles under contrasting logging regimes. Biol. Conserv. 144, 166–174.
Smith, W.B., 2002. Forest inventory and analysis: a national inventory and monitoring program. Environ. Pollut. 116, S233–S242.
Soverel, N.O., Perrakis, D.D.B., Coops, N.C., 2010. Estimating burn severity from Landsat dNBR and RdNBR indices across western Canada. Remote Sens. Environ. 114, 1896–1909.
Stueve, K.M., Perry, C.H., Nelson, M.D., Healey, S.P., Hill, A.D., Moisen, G.G., Cohen, W.B., Gormanson, D.D., Huang, C., 2011. Ecological importance of intermediate windstorms rivals large, infrequent disturbances in the northern Great Lakes. Ecosphere 2 (art2).
Tao, X., Yan, B.Y., Wang, K., Wu, D.H., Fan, W.J., Xu, X.R., Liang, S.L., 2009. Scale transformation of Leaf Area Index product retrieved from multiresolution remotely sensed data: analysis and case studies. Int. J. Remote Sens. 30, 5383–5395.
Tao, X., Liang, S.L., Wang, D.D., 2015. Assessment of five global satellite products of fraction of absorbed photosynthetically active radiation: intercomparison and direct validation against ground-based data. Remote Sens. Environ. 163, 270–285.
Tao, X., Liang, S.L., He, T., Jin, H.R., 2016. Estimation of fraction of absorbed photosynthetically active radiation from multiple satellite data: model development and validation. Remote Sens. Environ. 184, 539–557.
Tao, X., Liang, S., Wang, D., He, T., Huang, C., 2018. Improving satellite estimates of the fraction of absorbed photosynthetically active radiation through data integration: methodology and validation. IEEE Trans. Geosci. Remote Sens. 56, 2107–2118.
Tewkesbury, A.P., Comber, A.J., Tate, N.J., Lamb, A., Fisher, P.F., 2015. A critical synthesis of remotely sensed optical image change detection techniques. Remote Sens. Environ. 160, 1–14.
Thomas, N.E., Huang, C.Q., Goward, S.N., Powell, S., Schleeweis, K., Hinds, A., 2011. Validation of North American forest disturbance dynamics derived from Landsat time series stacks. Remote Sens. Environ. 115, 19–32.
Townshend, J.R., Masek, J.G., Huang, C., Vermote, E.F., Gao, F., Channan, S., Sexton, J.O., Feng, M., Narasimhan, R., Kim, D., Song, K., Song, D., Song, X.-P., Noojipady, P., Tan, B., Hansen, M.C., Li, M., Wolfe, R.E., 2012. Global characterization and monitoring of forest cover using Landsat data: opportunities and challenges. Int. J. Digital Earth 5, 373–397.
Tucker, C.J., 1979. Red and photographic infrared linear combinations for monitoring vegetation. Remote Sens. Environ. 8, 127–150.
Wilson, E.H., Sader, S.A., 2002. Detection of forest harvest type using multiple dates of

Landsat TM imagery. Remote Sens. Environ. 80, 385–396.
Woodcock, C.E., Allen, R., Anderson, M., Belward, A., Bindschadler, R., Cohen, W., Gao, F., Goward, S.N., Helder, D., Helmer, E., Nemani, R., Oreopoulos, L., Schott, J., Thenkabail, P.S., Vermote, E.F., Vogelmann, J., Wulder, M.A., Wynne, R., 2008. Free access to Landsat imagery. Science 320, 1011.
Wulder, M., 1998. Optical remote-sensing techniques for the assessment of forest inventory and biophysical parameters. Prog. Phys. Geogr. 22, 449–476.
Wulder, M.A., White, J.C., Loveland, T.R., Woodcock, C.E., Belward, A.S., Cohen, W.B., Fosnight, E.A., Shaw, J., Masek, J.G., Roy, D.P., 2016. The global Landsat archive: status, consolidation, and direction. Remote Sens. Environ. 185, 271–283.
Xu, X.R., Fan, W.J., Tao, X., 2009. The spatial scaling effect of continuous canopy Leaves Area Index retrieved by remote sensing. Sci. China Ser. D Earth Sci. 52, 393–401.
Zhao, F., Huang, C., Zhu, Z., 2015. Use of vegetation change tracker and support vector machine to map disturbance types in greater yellowstone ecosystems in a 1984–2010 Landsat time series. IEEE Geosci. Remote Sens. Lett. 12, 1650–1654.
Zhao, F., Huang, C., Goward, S.N., Schleeweis, K., Rishmawi, K., Lindsey, M.A., Denning, E., Keddell, L., Cohen, W.B., Yang, Z., Dungan, J.L., Michaelis, A., 2018. Development of Landsat-based annual US forest disturbance history maps (1986–2010) in support of the North American Carbon Program (NACP). Remote Sens. Environ. 209, 312–326.
Zhu, Z., Woodcock, C.E., Olofsson, P., 2012. Continuous monitoring of forest disturbance using all available Landsat imagery. Remote Sens. Environ. 122, 75–91.